

Spatial distribution of liposome encapsulated tin etiopurpurin dichloride (SnET2) in the canine prostate; Implications for computer simulation of photodynamic therapy.

JACEK ANIOLA^{1,5}, STEVEN H. SELMAN¹⁻³, LOTHAR LILGE⁴, RICK KECK¹, JERZY JANKUN¹⁻³.

¹Urology Research Center, ²Department of Urology, ³Department of Physiology and Molecular Medicine, Medical College of Ohio, 3065 Arlington Ave., Toledo, OH 43614-5807, USA; ⁴Ontario Cancer Institute, Princess Margaret Hospital, 610 University Ave., Toronto, ON W5G 2W9, Canada.

Received October 21, 2002; Accepted December 5, 2002

Abstract. Photodynamic therapy (PDT) is minimally invasive treatment that can be employed in many human diseases including prostate cancer. PDT for prostate cancer depends on the sequestration of a photosensitizing drug within the glandular tissue. The photosensitizer is subsequently activated by light (usually from a laser) and the active drug destroys tissue. Since prostate cancer is a multi-focal disease, PDT must ablate the glandular prostate completely. This will depend on precise placement of light sources in the prostate and delivery of a therapeutic light dose to the entire gland. Also, sources of light and their spatial distribution must be tailored to each individual patient. The uniform, therapeutic light distribution can be achieved by interstitial light irradiation. In this case, the light is delivered by diffusers placed within the substance of the prostate parallel to the urethra at a distance optimized to deliver adequate levels of light and to create the desired photodynamic effect. To help achieve the uniform light distribution throughout the prostate we have developed a computer program that can determine treatment effects. The program predicts the best set of parameters and the position of light diffusers in space, and displays them in graphical or in numerical form assuming fixed attenuation coefficient. The two parameters of greatest importance in the computer simulation are attenuation coefficient and critical fluence. Both depend on the concentration of active drug within the prostate gland. It is necessary to know the nature of the spatial distribution of photosensitizer within the prostate to execute computer modeling of PDT with high precision.

We found that the concentration of SnET2 is heterogeneous in nature, and is higher in the proximity of the glandular capsule. It is clear therefore that any future attempts of computerized modeling of this procedure must take into consideration the uneven sequestration of photosensitizer and the consequential asymmetrical necrosis of the prostate.

Introduction

The widespread use of the PSA test as an adjunct to digital rectal examination has led to an increase in the diagnosis of prostate cancer in its early stages. Treatment of organ confined prostatic cancer includes radical prostatectomy, external beam radiotherapy, brachytherapy and cryosurgical ablation. Results from all these are favorable at least in terms of short outcomes. Still, with T1c disease, 30% of patients will have biochemical failure within 5 years of treatment. Clearly novel methods of prostate cancer treatment are needed. One such novel treatment is Photodynamic Therapy.

Photodynamic Therapy (PDT) is an emerging minimally invasive treatment that can be employed in many human diseases including prostate cancer (1-6). Photodynamic therapy for prostate cancer depends on the sequestration of a photosensitizing drug within the glandular tissue (7, 8). The photosensitizer is subsequently activated by high-energy light (usually from a laser) and the active drug destroys tissue with a sufficient high concentration of photosensitizer. Since prostate cancer is a multi-focal disease, PDT must ablate the glandular prostate completely. Complete glandular ablation will depend on precise placement of light sources in the prostate and delivery of a therapeutic light dose to the entire gland. The prostate is irregular in shape, with different dimensions so that transurethral light delivery that is cylindrical in distribution cannot be used for the treatment of the majority of prostate cancers. Additionally, most cancers are located in the peripheral zone of the prostate, an area unlikely to be reached by transurethrally delivered light. Sources of light and their spatial distribution must be tailored to each individual patient. More uniform, therapeutic light distribution can be achieved by interstitial light irradiation. In this case, the light is delivered by diffusers placed within the substance of the prostate parallel to the urethra at a distance optimized to deliver adequate levels of light and to create the desired photodynamic effect. To help

Address correspondence/reprint request to: Jerzy Jankun, Director of Urology Research Center, Department of Urology, Department of Physiology and Molecular Medicine, Medical College of Ohio, 3065 Arlington Ave., Toledo, OH 43614-5807, USA
phone: 419-383-3691, FAX 419-383-3168,
e-mail:jjankun@mco.edu,
<http://golemxiv.dh.mco.edu/~jerzy/>

⁵present address: Department of Hygiene and Human Nutrition, A. Cieszkowski University, 31 Wojska Polskiego, Poznan, Poland.

achieve uniform light distribution throughout the prostate we have developed a computer program that can determine treatment effects by calculating the distribution of light energy depending on the number of light sources placed in the prostate, their position in the gland, the dimension of the prostate, and the tissue attenuation coefficient. A patient's three-dimensional prostate model is built based on ultrasound images. The computer program predicts the best set of parameters and position of light diffusers in space displaying them in graphical or numerical form (9).

The two parameters of greatest importance in the computer simulation are attenuation coefficient (absorption and scatter coefficient of light) and critical fluence (minimum energy of light needed to kill prostatic tissue). Both depend on the concentration of active drug within the prostate gland (9). It is therefore necessary to know the nature of the spatial distribution of photosensitizer within the prostate to execute computer modeling of photodynamic therapy with high precision.

Materials and Methods

Algorithm of the light distribution in the prostate. The distribution of light energy fluence Φ_1 in J cm^{-2} , around the cylindrical fiber, placed in a highly scattering medium, such as the prostate gland, can be expressed using the solution of the diffusion equation in cylindrical coordinates:

$$\Phi_1 = \Phi_0 \exp(-r \mu_{\text{eff}}) \quad \text{i)}$$

where: Φ_0 is the energy fluence at the light source, μ_{eff} is the effective attenuation coefficient in cm^{-1} that describes absorbing and scattering properties of the prostate, and r is the distance from the delivery fiber in cm (10-12), μ_{eff} is described by equation:

$$\mu_{\text{eff}} = (3 \mu_a (\mu_a + \mu_s))^{-1} \quad \text{ii)}$$

where: μ_a is light absorption coefficient, μ_s is light scattering coefficient. To determine light distribution within the gland, a map of the prostate and surrounding space was created. Each voxel (three-dimensional pixel) is described by x_a , y_b , and z_c coordinates. Each voxel's light fluence was calculated as a sum of light fluence from each source:

$$\Phi_{x,y,z} = \Phi_1 \exp(-r_1 \mu_{\text{eff}}) + \Phi_2 \exp(-r_2 \mu_{\text{eff}}) + \dots \quad \text{iii)}$$

where: $\Phi_{x,y,z}$ is the light fluence at voxel x_a , y_b , z_c at distance: r_1, r_2, \dots , from: 1, 2, \dots , light source with initial light fluence of: Φ_1, Φ_2, \dots

Photosensitizer. Tin etiopurpurin dichloride (Frontier Scientific, Inc., Logan, UT) was used as the tissue photosensitizer. SnET2 lipid emulsion was prepared using a chloroform dissolved mixture of: 200 mg of SnET2, 1g of 1,2-Dioleoyl-sn-Glycero-3-Phosphocholine, 1g of 1,2-Dimyristoyl-sn-Glycero-3-Phosphocholine, 100 mg of 1,2-Dioctanoyl-sn-Glycero-3-Phosphocholine (all from Avanti Polar-Lipids, Inc., Alabaster, AL), 100 mg of 1,2-Dilauroyl-sn-Glycero-3-Phosphocholine

(Avanti) and 200 mg of (\pm)- α -Tocopherol (Sigma, St. Louis, MO). The mixture was rotary evaporated using high purity argon and desiccated under vacuum overnight. The remaining thin layer of lipids was homogenized in 100 ml of 0.9% NaCl solution by sonication, using a Sonic Dismembrator, Model 100 (Fisher Scientific, Pittsburgh, PA). This liposome emulsion was then extruded several times using a series of ISOPORE™ Polycarbonate Membrane Filters: 1.2 μm , 0.8 μm , 0.6 μm , 0.4 μm (Millipore Corporation, Bedford, MA) and finally with Fisherbrand® sterile 0.2 μm syringe filters (Fisher Scientific, Pittsburgh, PA). The recovery of SnET2 by this method was about 50%.

Liposome size distribution. Particle size distribution was determined by Science and Technology Laboratory, Miami, FL using a Beckman Coulter N4 Plus Submicron Particle Size Distribution Analyzer utilizing photon correlation spectroscopy. The samples were dispersed in DI-water filtered with a 20 nm filter and analyzed at the 90° angle at a temperature of 25°C for 900 seconds (13, 14).

Animals. Adult canines were housed 1 per cage and given free access to water and canine chow (Purina chow, Ralston Purina Corp., Richmond, IN). Animals were injected with SnET2 (1.0 mg/kg) as a lipid emulsion vehicle *via* the antecubital vein 24 hours prior to light treatment.

Treatment light source and delivery. A 6-Channel 665nm/600mW Laser System (Phototonics Research, Ontario, Canada) with a LDC-3908 Laser Diode Controller (ILX Lightwave, Bozeman, MT) and computer control was used as a light (665 nm) source. Laser light was delivered to the prostate fossa *via* a 400 μm optical fiber fitted with a 2.0 cm flexible cylindrical diffuser tip (PDT System, Inc., Santa Barbara, CA).

Prostate PDT treatment. Animals (n=5) were anesthetized using an *i. v.* administered cocktail of Xylazine (1 mg/kg body wt.) and Ketamine (22 mg/kg body wt.), followed by intubation and halothane/oxygen inhalation. Each animal underwent a bowel preparation and had the bladder drained using a urinary catheter. The perineum was scrubbed with Betadine. Under TRUS (transrectal ultrasound imaging), 18G brachytherapy needles (Cook Urological, Spencer, Indiana) were introduced transperineally and placed within the right lobe of the prostate. The brachytherapy needles were used for introduction of laser diffusers. Once the laser fiber tip was positioned within the prostatic fossa, the prostate was treated with 200 joules per cm. (200 mW/cm, 1000 seconds) of laser light.

Twenty-four hours following PDT each animal was euthanized with an *i.v.* injection of Beuthanasia-D. At necropsy the prostate was removed and the right and left lobes were separated. The left prostatic lobe was frozen and utilized for pharmacokinetic studies and the right lobe was fixed in phosphate buffered formalin and paraffin processed for histologic evaluation and measurement of the necrotic front.

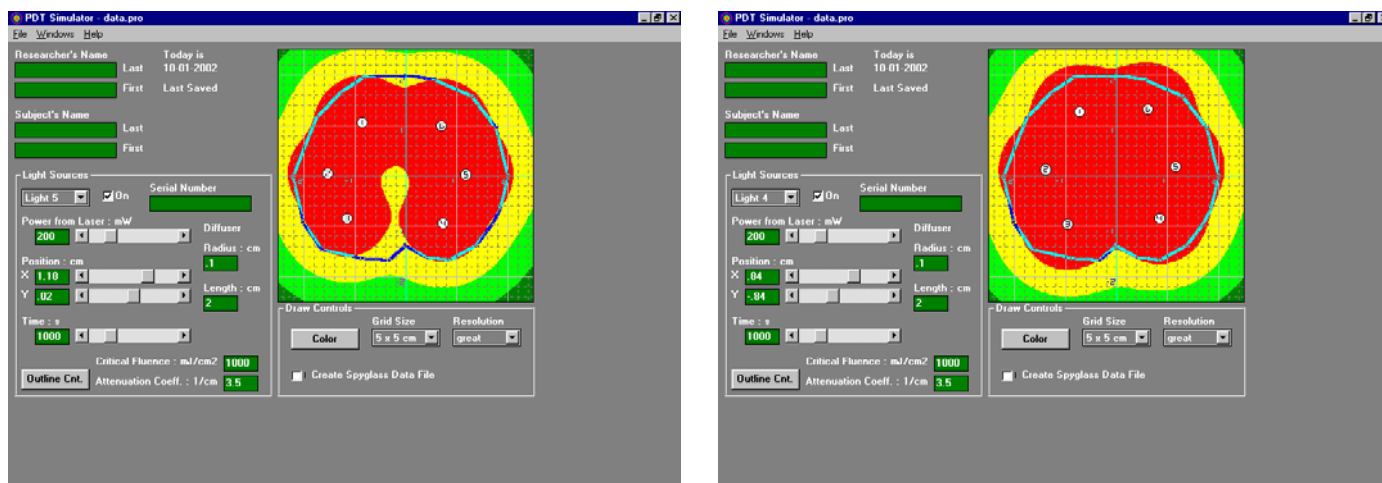


Fig. 1. Light fluence in a cross-section of the prostate (left). The center of the section (green and yellow) indicates that the entire prostate was not exposed to the minimum energy needed for activation of the photosensitizer. Some adjustments are needed such as longer exposure or higher power of light. After suitable adjustments (red color) filled the entire space of the prostate, no "cold" untreated areas are visible.

Photosensitizer extraction. Tissue samples were removed from the prostate, urinary bladder and rectum. All samples were processed under the protection of blue-green filtered light: RoscoLux 89 Moss Green and RoscoLux 370 Italian Blue Filters (Rosco LA, Hollywood, CA). The prostatic lobes were cut into 5 mm thick slices. Each slice was placed on a grid, photographed, frozen and cut into 5mm cubes. The extraction data for each cube was used to create a map depicting sensitizer concentration of each slice.

Photosensitizer extraction was performed using a modification of published techniques (15, 16). Briefly, tissue samples were weighed and homogenized with a biohomogenizer: Tissue-Tearor (Biospec Products, Inc., Bartlesville, OK) in 9% acetic acid. After the addition of a 3:1 ethyl acetate: glacial acetic acid mixture, samples were mixed vigorously. Saturated sodium acetate was added and mixed again. The samples were then allowed to sit overnight to equilibrate/extract. After centrifugation, the ethyl acetate layer, containing the photosensitizer, was removed and its concentration was determined using fluorescence detection (Spectrofluorometer Mark I, Farrand Optical Co., Inc., New York, NY).

Statistical analysis. The one-way analysis of variance was run on the extraction data results using SigmaStat (Jandel Scientific Software, San Rafael, CA).

Results and Discussion

Computer simulation of PDT. As described in the M&M section and in previous work, formulas 1 and 3 were used to develop a 2D and 3D model of treatment. This computer program calculates the distribution of energy fluence depending on the number of light sources placed in the prostate, their position in the gland, the dimension of the prostate, and their attenuation coefficient (9). It calculates the power and the position of the light sources that were thought to be needed to destroy malignant tissues. As shown in Figure 1 the computer predicts the best set of parameters and the position of light

diffusers in space, and displays them in graphical or in numerical form assuming fixed μ_{eff} of the PDT treatment.

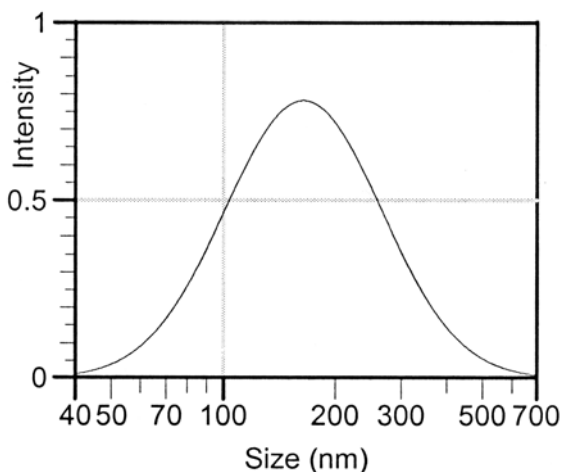


Fig. 2. Typical size distribution of SnET2 bearing liposomes.

Computer simulation was done on the assumption that spatial distribution of photosensitizer within the prostate was uniform. If that parameter is not the same for different parts of gland it must be measured and this variable must be incorporated into the computer program.

Delivery of active compound to the organ of interest depends on many factors including size of the liposomes (17, 18). To provide uniformity during these experiments the size of liposomes was measured. As shown in Figure 2 the mean diameter of liposomes was 178 ± 48 nm. Throughout the experiment the liposome diameter was randomly measured to insure each preparation was within the limits of this value.

SnET2 concentration was measured in the non- light treated (left) prostatic lobes. Each slice was divided into 3 groups, depending on their location in relationship to the urethra and prostatic capsule as shown in Figure 3. Group E (external) being the outermost layer near the capsule, group U (urethral) being the inner most layer around the urethra and group I (internal) being the layer in between.

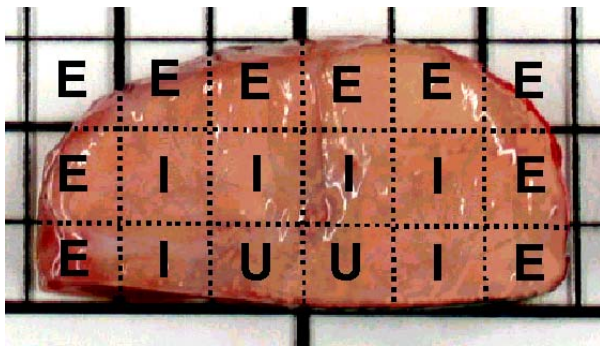


Fig. 3. Prostate slice used for SnET2 extraction, illustrating how cubes were labeled for mapping. Group E (external) being the outermost layer near the capsule, Group U (urethral) being the inner most layer around the urethra and Group I (internal) being the layer in between.

Table 1. Tissue distribution of SnET2 [$\mu\text{g/g}$] in animals that received 1.0 mg/kg of SnET2 (mean \pm SD)

Animal No.	Prostate	Rectum	Bladder
2956	1.58 \pm 0.49	0.48 \pm 0.05	0.31 \pm 0.03
	n = 91	n = 3	n = 3
2958	1.63 \pm 0.67	0.52 \pm 0.04	0.32 \pm 0.01
	n = 85	n = 3	n = 3
2960	0.81 \pm 0.53	0.27 \pm 0.01	0.41 \pm 0.05
	n = 55	n = 3	n = 3
2962	1.70 \pm 0.76	0.48 \pm 0.03	0.36 \pm 0.05
	n = 70	n = 3	n = 3
2965	1.15 \pm 0.65	0.32 \pm 0.08	0.23 \pm 0.01
	n = 53	n = 3	n = 3
Mean	1.43 \pm 0.70	0.44 \pm 0.09	0.30 \pm 0.06
	n = 354	n = 15	n = 15

The control animal not injected with photosensitizer showed no response to light treatment. Samples from three slices (n=74) were analyzed for SnET2 content. No detectable photosensitizer was found.

SnET2 levels for prostate, rectum and bladder mucosa are shown in Table 1. Within animals injected with 1.0 mg/kg of SnET2, the mean photosensitizer level for the prostate was 1.43 $\mu\text{g/g}$. The rectum and bladder tissues contained less photosensitizer than did the prostate. With the exception of dog 2960 the specific uptake of SnET2 in the rectum contained 30 \pm 2% of the content found in the related prostate, while the bladder mucosa contained 20 \pm 1%. This low content of photosensitizer will help to reduce the risk of photodynamic injury to these organs when the prostate is treated. The average tissue distribution of SnET2 found in the current set of experiments is similar to that obtained and reported previously using an emulsion (5).

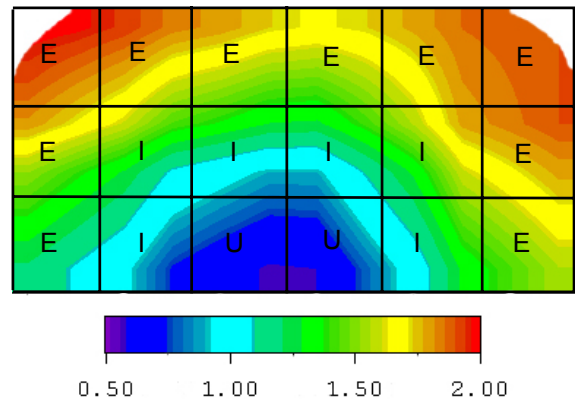


Fig 4. Typical interpolated rainbow image of SnET2 concentration map in prostate slice.

Table 2 Pairwise multiple comparison of groups means - differences of means [$\mu\text{g/g}$]; statistically significant differences ($p < 0.05$) are marked by asterisks.

Canine No.	E vs. U	E vs. I	I vs. U
2956	0.85 *	0.03	0.82 *
2958	1.18 *	0.14	1.04 *
2960	0.77 *	0.44 *	0.33
2962	1.40 *	0.33	1.08 *
2965	1.14 *	0.46 *	0.68 *
All data	1.11 *	0.24 *	0.87 *

However, no information regarding spatial distribution of SnET2 in the prostate has been previously reported. In the current study, differences in photosensitizer distribution throughout the prostate were noticed when extraction data was mapped for each prostate slice. The drug concentration was noticeably lower in the center of the organ (near the urethra) and higher as one goes toward the prostatic capsule. Figure 4 shows a SnET2 concentration gradient map for a typical slice of prostate.

The extraction data from all five canines was compiled and separated into 3 groups, according to their location within the prostate: U (around the urethra), I (internal), E (external, near the capsule). Using the one-way analysis of variance, the means of U, I and E groups were compared for all canines separately and together, pairwise multiple comparison differences of means are shown in Table 2. In all cases there were significant differences between the SnET2 concentrations found in the inner part of prostate, around the urethra and the outermost layer near the capsule.

When comparing the data from all five animals, as shown in Figure 5, significant ($p < 0.05$) differences between all three groups (U, n = 58; I, n = 94; and E, n = 202) were found. Differences between E vs. U; E vs. I; and I vs. U were statistically significant ($p < 0.0001$).

Additionally, in animals treated with SnET2 and laser light differences in radii of the necrotic front around the diffuser site

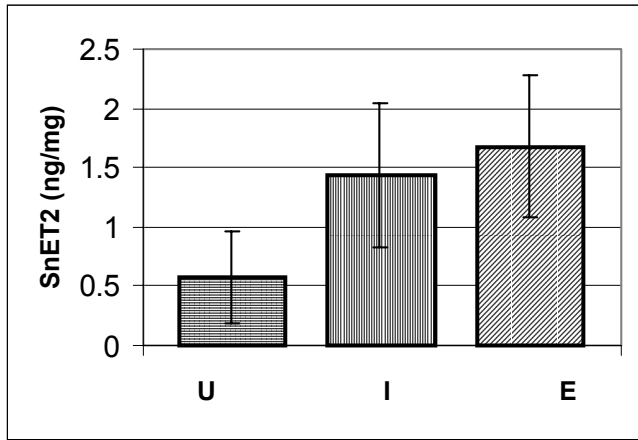


Fig. 5. SnET2 concentration [$\mu\text{g/g}$] in non light treated (left) prostate lobes, divided into groups- according to their location (mean \pm SD); group E (external), U (urethral) and I (internal).

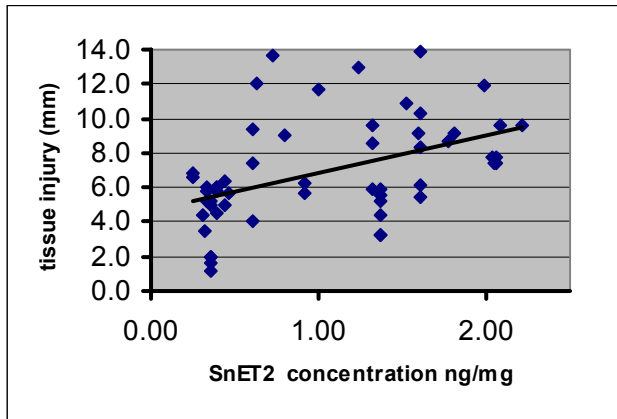


Fig. 6. Relationship between SnET2 concentration ($\mu\text{g/g}$) and the radius of the tissue injury (mm).

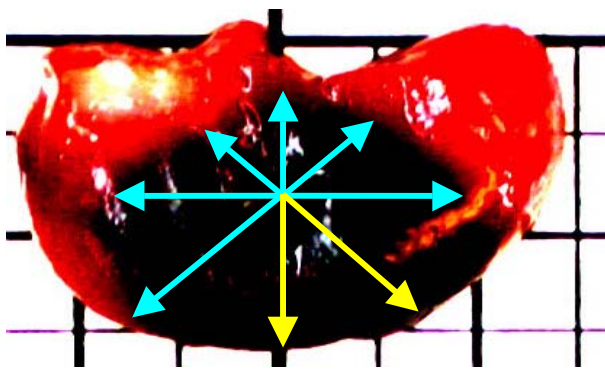


Fig. 7. Contrast enhanced photo of the light treated prostate slice. Using the corresponding TRUS images as a reference, the diffuser location was marked on the photographs of the prostate slices and the distances in eight directions to the hemorrhagic (necrotic) front were measured and recorded. Measurements within these slices where the hemorrhagic front reached the prostatic capsule were not included (yellow arrows). Dark area represents necrotic tissue, red untreated part of gland.

were noted (Figure 6). When comparing the SnET2 concentration of the left prostatic lobe cubes corresponding to each radial measurement of the necrotic front in the right lobe, the linear regression analysis showed a statistically significant ($p < 0.05$, $R^2 = 0.2077$, $y = 2.1542x + 4.7122$) relationship between the SnET2 concentration (x , $\mu\text{g/g}$) and the radius of the tissue injury (y , mm), as shown in Figure 7.

Only slices within the treated area of the prostate were used in these determinations. Measurements within these slices where the hemorrhagic front reached the prostatic capsule were not included –as represented by the yellow arrows in figure 6. These determinations were made under the assumption that the right and left halves of each prostate slice mirror each other in SnET2 uptake and have similar light characteristics.

All these data indicate that the concentration of the photosensitizer, SnET2 in the prostate is heterogeneous in nature, and is higher in the proximity of the glandular capsule. The lower amount of SnET2 in the urethral region could be beneficial since it is preferred to spare this part of prostate. It is clear also that any future attempts of computerized modeling of this minimally invasive procedure must take into consideration the uneven sequestration of photosensitizer and the consequential asymmetrical necrosis of the prostate.

Acknowledgments

This work was supported in part by grants from: NIH, R01 CA90524, and Frank D. Stranahan Endowment Fund for Oncological Research.

References

1. Chang, SC, Buonaccorsi, G, MacRobert, A, and Bown, SG Interstitial and transurethral photodynamic therapy of the canine prostate using meso-tetra-(m-hydroxyphenyl) chlorin. *Int J Cancer*, 67: 555-562, 1996.
2. Chen, Q, Wilson, BC, Shetty, SD, Patterson, MS, Cerny, JC, and Hetzel, FW Changes in in vivo optical properties and light distributions in normal canine prostate during photodynamic therapy. *Radiat Res*, 147: 86-91, 1997.
3. Gomer, CJ Photodynamic therapy in the treatment of malignancies. *Semin Hematol*, 26: 27-34, 1989.
4. Marcus, SL, Sobel, RS, Golub, AL, Carroll, RL, Lundahl, S, and Shulman, DG Photodynamic therapy (PDT) and photodiagnosis (PD) using endogenous photosensitization induced by 5-aminolevulinic acid (ALA): current clinical and development status. *J Clin Laser Med Surg*, 14: 59-66, 1996.
5. Selman, SH and Keck, RW The effect of transurethral light on the canine prostate after sensitization with the photosensitizer tin (II) etiopurpurin dichloride: a pilot study. *J Urol*, 152: 2129-2132, 1994.
6. Selman, SH, Keck, RW, and Hampton, JA Transperineal photodynamic ablation of the canine prostate. *J Urol*, 156: 258-260, 1996.
7. Fisher, AM, Murphree, AL, and Gomer, CJ Clinical and preclinical photodynamic therapy. *Lasers Surg Med*, 17: 2-31, 1995.
8. Kessel, D, Woodburn, K, Gomer, CJ, Jagerovic, N, and Smith, KM Photosensitization with derivatives of chlorin p6. *J Photochem Photobiol B*, 28: 13-18, 1995.
9. Jankun, J, Zaim, A., Jankun-Kelly, M., Keck, R. W. Selman, S. H. Computer Model for Photodynamic Therapy of the Prostate. *Proceedings of SPIE*, 3907: 222-228, 2000.
10. Jacques, SL Light distributions from point, line and plane sources for photochemical reactions and fluorescence in turbid biological tissues. *Photochem Photobiol*, 67: 23-32, 1998.
11. Sassaroli, A, Martelli, F, Imai, D, and Yamada, Y Study on the propagation of ultra-short pulse light in cylindrical optical phantoms. *Phys Med Biol*, 44: 2747-2763, 1999.
12. Tromberg, BJ, Svaasand, LO, Fehr, MK, Madsen, SJ, Wyss, P, Sansone, B, and Tadir, Y A mathematical model for light dosimetry in photodynamic destruction of human endometrium. *Phys Med Biol*, 41: 223-237, 1996.
13. Mobed, M, Nishiya, T, and Chang, TM Purification and characterization of liposomes encapsulating hemoglobin as potential blood substitutes. *Biomater Artif Cells Immobilization Biotechnol*, 20: 53-70, 1992.
14. Kolchens, S, Ramaswami, V, Birgenheier, J, Nett, L, and O'Brien, DF Quasi-elastic light scattering determination of the size distribution of extruded vesicles. *Chem Phys Lipids*, 65: 1-10, 1993.
15. Frazier, DL, Barnhill, MA, Vodinh, T, Legendre, AM, and Overholt, BF Comparative pharmacokinetics of the photosensitizer tin-etiopurpurin in dogs and rats. *J Vet Pharmacol Ther*, 15: 275-281, 1992.
16. Kessel, D, Garbo, GM, and Hampton, J The role of lipoproteins in the distribution of tin etiopurpurin (SnET2) in the tumor-bearing rat. *Photochem Photobiol*, 57: 298-301, 1993.
17. Moghimi, SM and Patel, HM Modulation of murine liver macrophage clearance of liposomes by diethylstilbestrol. The effect of vesicle surface charge and a role for the complement receptor Mac-1 (CD11b/CD18) of newly recruited macrophages in liposome recognition. *J Control Release*, 78: 55-65, 2002.
18. Hong, MS, Lim, SJ, Lee, MK, Kim, YB, and Kim, CK Prolonged blood circulation of methotrexate by modulation of liposomal composition. *Drug Deliv*, 8: 231-237, 2001.